Effect of Nozzle Outlet Geometry and Impinged Surface Geometry on Erosion Caused by Cavitating Jets for Hydraulic Equipment

Toshiharu Kazama*, Kento Kumagai and Yukihito Narita

**College of Design and Manufacturing Technology, Muroran Institute of Technology, 27-1, Mizumoto-cho, Muroran, Hokkaido, 050-8585, Japan.*

Corresponding author: E-mail: kazama@mmm.muroran-it.ac.jp

ABSTRACT

In order to investigate cavitation erosion in hydraulic equipment, an experiment was conducted using a submerged cavitating jet rig. The erosive effects of various nozzle outlet geometries and the impinged surface geometries were examined using six type nozzle holders and three spacers or two cylindrical walls in the experiment. The upstream pressure was set at 10.1 MPa and the cavitation number was between 0.02 and 0.04. A petroleum-based hydraulic oil with a viscosity grade of 32 was used as the test liquid and the temperature was maintained at 40°C. Aluminum alloy specimens of each 15 mm in diameter were used. The results indicate that a concave-type surface reduced erosion considerably, whereas convex-type surfaces tended to enhance erosion. Mass loss of the specimens decreased for specific nozzle outlet geometries. The size of a ring-like eroded region was the smallest for concave-type specimens. Erosion tended to increase for smaller cavitation numbers.

Keywords: Cavitation, Erosion, Geometry, Jet, Oil

INTRODUCTION

Cavitation (Knapp et al, 1970) and cavitation erosion (Plesset and Devine, 1966) is a serious problem affecting fluid machinery such as valves and pumps. Impingement of a cavitating jet of highly pressurized liquids is the main cause of erosion in hydraulic equipment. It results from the collapse of bubbles at or near the solid boundaries. Erosion caused by cavitating jets should be reduced to extend the life of hydraulic systems.

To evaluate the erosion caused by impingement of a cavitating jet, Lichtarowicz (1972) proposed a submerged cavitating jet apparatus. Using prototypes based on his concept, subsequently, Kleinbreuer (1977), Yamaguchi and Shimizu (1987), and others have studied jet-cavitation erosion.

The authors and collaborators have investigated cavitation erosion behavior by applying a jet cavitation rig to oil-based and water-based hydraulic equipment. The effects of various fluids and materials on erosion have been examined.

The parameters tested included upstream pressure, pressure pulsation, cavitation number, fluid types such as tap water, mineral oils, and water-glycol type fluids (Kazama and Shinizu, 2007), size of nozzles and their outlet geometries (Kazama and Yamaguchi, 2000), specimen configuration, material properties of specimens, and comparison of test methods (Yamaguchi et al., 2001).

Based on those results, the authors specifically examined how to reduce erosion from cavitating jets passively (Kazama and Miura, 2007). The effects of nozzle outlet geometry and impinged surface geometry were examined for tap water (Kazama et al., 2009). The experiment reported in this paper uses a jet cavitation rig with hydraulic oil to evaluate the influence of nozzle outlet geometry and the impinged surface geometry on erosion. The effect of cavitation number is also investigated.

TEST RIG AND EXPERIMENTAL PROCEDURE

Test Method

The apparatus and test procedures used for this work were similar to those prescribed in ASTM standards (1995), but with partially differing geometry and test conditions. The relative deviation of the tests used here from the ASTM standards is similar to that described in Ref. (Yamaguchi and Shimizu, 1987).

Experimental Apparatus

The hydraulic circuit for testing erosion with hydraulic oil included a test chamber, a positive displacement pump with an electric motor, accessories including valves, a cooler, a filter, and a reservoir, and instruments including pressure gages and thermometers. The pump was a vane-type hydraulic pump and its maximum operating pressure and discharge were 40 MPa and 2.3×10^{-4} m^3/s, respectively. An inline filter with a nominal filtration size of 3 μm was used to remove contaminants from the test liquid. A cooler capable of maintaining a desired liquid temperature was also installed.

The test chamber arrangement is presented in Fig. 1. The stainless steel chamber included a long-orifice nozzle, its holder, the specimen, its mount, and spacers. The 80-mm-diameter inner chamber was cylindrical.

Two transparent windows were provided at both sides of the chamber so that the cavitating jet could be observed and photographed. Annular spacers with various thickness enabled adjustment to an arbitrary standoff distance *L*. The nozzle diameter and length were 1.0 and 4.0 mm, respectively. The nozzle was bored cylindrically; its inlet was manufactured carefully to provide a very sharp entry edge.

Configuration Close to Outlets of Nozzle

The nozzle was fixed using holders of various geometries, as presented in Fig. 2, for passive control of the cavitating jet flowing out from the nozzle. This figure shows the jet flow issued upward. The six holders tested are referred to as ϕ3S, ϕ3T, M3, ϕ6S, ϕ3S-6, and ϕ3S-C. Holder ϕ3S had a straight through hole

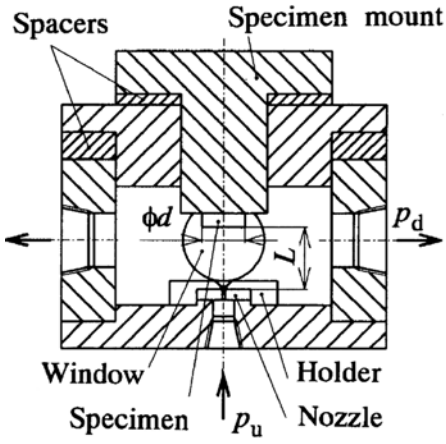

Figure 1. Schematic of the test chamber.

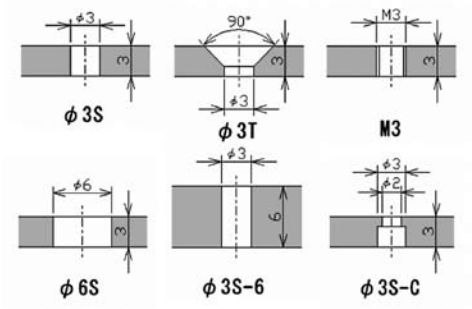

Figure 2. Configuration of nozzle outlets.

of 3-mm diameter and 3-mm length. Holder ϕ3T had a tapered flow path with an angle of 90°. The holder M3 path was tapped with an M3 screw thread. Holder ϕ6S had a 6-mm-diameter hole and 3-mm length. Holder ϕ3S-6 had a 3-mm-diameter hole and a 6-mm flow path. Holder ϕ3S-C had a 3-mm-diameter hole contracted to 2 mm at the outlet of the path, thereby forming a small chamber at the nozzle outlet.

Configuration Close to Impinged Surfaces of Specimen

A cylindrical wall with height H was placed onto the specimen mount, which fenced the specimen off circumferentially, so that the impinged surface of the cavitating jet was formed as a concave shape. Alternatively, a small spacer with the same diameter of the specimen was inserted between the specimen and the mount, as presented in Fig. 3. Attachment of the wall formed a concave shaped impinged surface, while insertion of the spacer formed a convex shaped impinged surface; thus, the flow field close to the impinged surfaces of the cavitating jets can be controlled passively. The height H was defined as $H = 0$ mm when the level of the specimen surface and the top of the cylindrical wall were the same. The height H was positive when the top of the wall was higher

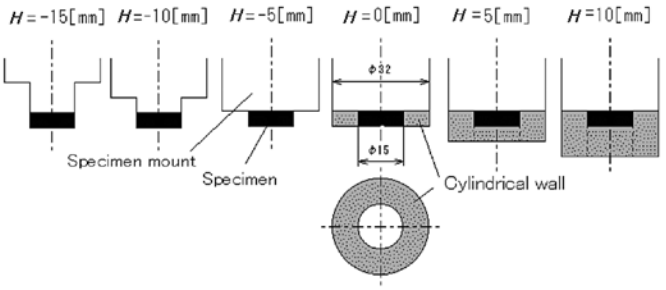

Figure 3. Configuration of the cylindrical wall and spacers close to the impinged surface of the specimen.

than the specimen surface, forming a concave shape; it was negative when the top of the wall was lower than the specimen surface level, forming a convex shape.

Specimens

Each specimen had a diameter of 15 mm. The specimens were made of A5056 aluminum alloy, as designated by Japanese Industrial Standards (JIS), which corresponds to AlMg5 in Deutsches Institut fur Normung (DIN). The physical and mechanical properties were the following: modulus of longitudinal elasticity 69.6 GPa, Vickers hardness 77 Hv, micro-Vickers hardness 98 Hmv, density 2730 kg/m^3, yield stress 124 MPa, breaking strength 272 MPa, tensile strength 223 MPa, breaking elongation 30.2%, and contraction of area 49.3%. The chemical composition was Cr: 0.07%, Cu: 0.01%, Fe: 0.09%, Mg: 4.53%, Mn: 0.08%, Si: 0.08%, Ti: 0.01%, Zn: 0.01%, and Zr < 0.01%.

Experimental Conditions

The liquid tested in this study was a mineral-oil-based hydraulic fluid with an ISO viscosity grade of 32 (32.6/5.49 mm^2/s at 40/100°C). By recirculating the test liquid and installing an inline cooler, the temperature T was maintained at T = 40±1°C. The upstream absolute pressure p_u was maintained at 10.1 MPa. The cavitation number σ was defined as the ratio of the downstream pressure p_d to the upstream pressure pu, i.e., $\sigma = p_d / p_u$; it was maintained between 0.02 and 0.04.

Test Procedure

Experiments were conducted under the following procedures. At the beginning of each test, the cylindrical wall height or the thickness of the spacer between the specimen and the mount, and the standoff distance L was set; the liquid temperature T was elevated. The specimen was mounted co-axially with the nozzle. The chamber was filled with the liquid. The remaining air and bubbles were then bled slowly from the chamber.

Pressurized liquid was supplied from a constant pressure source at pressure p_u. The submerged jet was cavitated through the nozzle and discharged into the

chamber at a constant pressure p_d. The cavitating jet was impinged upon the specimen surface. Upstream pressure pu and downstream pressure pd and liquid temperature T were monitored continuously and controlled precisely to maintain the experimental conditions during each test.

Pump operation was interrupted at regular intervals of 15 min in exposure periods of 1 h, by 30 min in the periods of 1-2 h, and of 1 h in periods longer than 2 h. The interruption for instrumentation was repeated during a specific period of up to 100 h.

At each interval, the specimen was removed carefully and rinsed sufficiently with normal hexane. The mass was determined using a precision balance with accuracy and sensitivity of 0.1 mg. The sectional profile of each eroded specimen's surface was recorded using a contact-type profilometer. Each eroded specimen's surface was photographed and observed.

The standoff distance L was defined as the distance from the edge of the nozzle outlet to the specimen surface, as indicated in Fig. 1. Using the annular spacers, L was increased from 15 mm to 30 mm in increments of 2.5 mm.

EXPERIMENTAL RESULTS AND DISCUSSION

Time Evolution of Mass Loss and Erosion Rate

Figures 4 and 5 depict the mass loss M and the erosion rate ER versus exposure time t. The loss M corresponded to the cumulative erosion and the rate ER to the interval erosion rate (using ASTM terminology). The cavitation number σ was 0.02. The wall height H was –5 mm when neither a cylindrical wall nor a spacer was installed. The standoff distance L was 25 mm, which was chosen where the mass loss M peaked at a specific distance (L_{max}) within the range under other conditions.

The mass loss M increased as the exposure time t proceeded. The variations of M were similar among nozzle outlets, although the absolute value of the loss M differed greatly. The difference in the loss M between ϕ3S and ϕ3S-C was of the order of 10^2, but the mass loss M for ϕ3S and ϕ3T was very similar.

For the various geometries of the nozzle outlets, the changes in the erosion rate ER versus exposure time t were markedly different; the rate of ER in the cases of ϕ3S and ϕ3T was large and maximized within a shorter exposure period. In this experimental condition, the maximum value of ER appeared within 12 h. In contrast, the rate ER in the cases of ϕ3S-6 and ϕ3S-C was much smaller than that for ϕ3S and ϕ3T. For those cases, the maximum rate ER was only weakly shown within 100 h.

To suppress cavitation erosion in the hydraulic equipment, therefore, the outlets where the cavitating jets discharged should be manufactured to a specific geometry, such as that of ϕ3S-6 or ϕ3S-C, to lengthen the flow path or to form a small chamber close to the nozzle outlet.

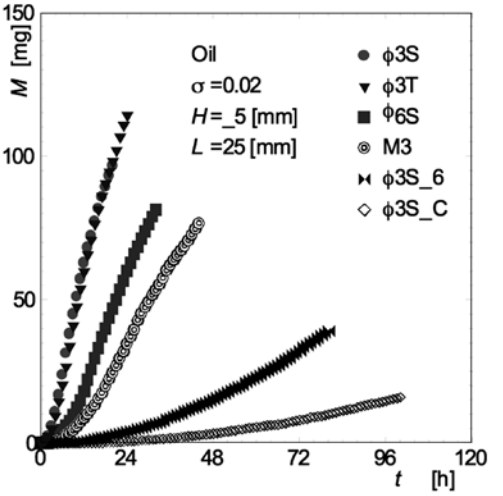

Figure 4. Mass loss M versus exposure time t for different nozzle outlets (H = –5 mm, L = 25 mm, σ = 0.02).

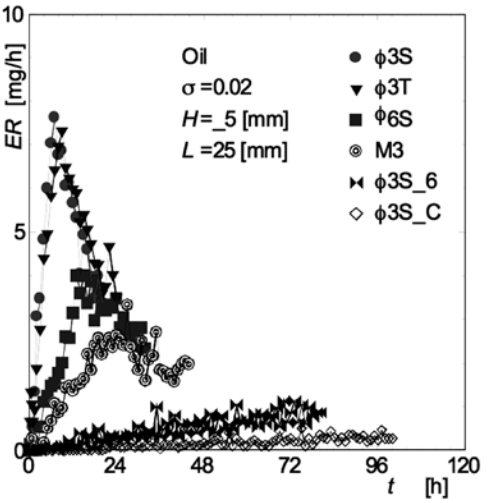

Figure 5. Erosion rate ER versus exposure time t for different nozzle outlets (H = –5 mm, L = 25 mm, σ = 0.02).

Effect of Height of the Cylindrical Wall

Figure 6 shows the eroded surfaces of the specimens for the case of the cylindrical wall height H between –15 mm and 10 mm. The specimen surface was eroded in a ring-like fashion. We observe that the convex surfaces (corresponding to H = –15, –10, and –5 mm) were strongly eroded, and the flat surface (H = 0 mm) was somewhat less eroded. In contrast, the convex surfaces (H = 5 and 10 mm) were markedly less eroded. The region damaged by erosion with positive H was small, whereas that with negative H was large.

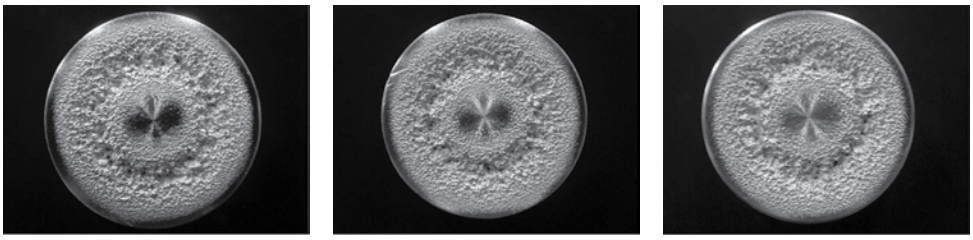

(a) H = –15 mm (b) H = –10 mm (c) H = –5 mm

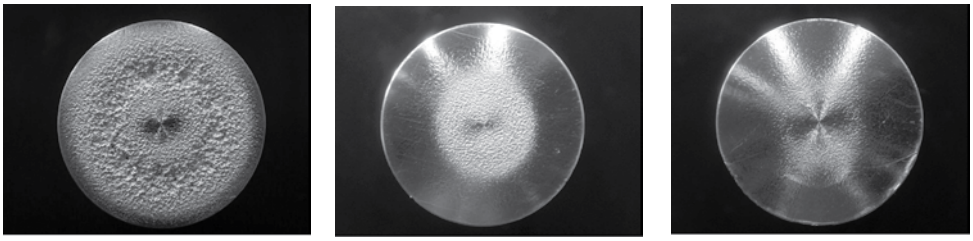

(d) H = 0 mm (e) H = 5 mm (f) H = 10 mm

Figure 6. Eroded surfaces of specimens for varying wall height H (ϕ3S, σ = 0.02, L = 25 mm, t = 8 h).

The progress and the strength of erosion were evaluated quantitatively, besides mass loss, on the basis of the diameters of the ring-like eroded region, which are defined by the inner diameter D_i, the outer diameter D_o, and the diameter D at the deepest valley.

Figure 7 presents the inner diameter D_i and outer diameter D_o of the eroded region and the deepest valley diameter D of the specimen surfaces for ϕ3S, ϕ6S, M3, and ϕ3S-C. As the exposure time t proceeded, D_i increased and D_o decreased. The diameters D_i and D_o became gradually asymptotic as the exposure time t proceeded. The diameters of ϕ3S, ϕ6S, and M3 became constant within a shorter period of 24 h, although the diameters, in particular D_o of ϕ3S-C, were gradually asymptotic. Comparing with the results shown in Fig. 4, the time taken for saturation of the diameters was strongly related to the specimen's mass loss: the larger the mass loss, the shorter the saturation time.

Effect of Cavitation Number

Figure 8 shows the eroded surfaces for cavitation numbers 0.02, 0.03, and 0.04 under the condition that the height was set at –10 mm. It can be observed that the damage to the specimen surfaces decreased as the value of σ increased.

Figures 9 and 10 plot the effect of the wall height H and the cavitation number σ on the mass loss M and the erosion ring diameter D, respectively. For convex surfaces (H < 0), the mass loss M was large; for a flat surface (H = 0), M was somewhat smaller, and for concave surfaces (H > 0), M became

remarkably small. The effects of the height H on the loss M were noticeable for larger values of σ.

The diameters D and D_o were larger for smaller values of σ, while the diameter D_i was barely affected by it. In other words, as the height H increased and became positive, such that the surface was deeply concave, D_o decreased and D_i increased.

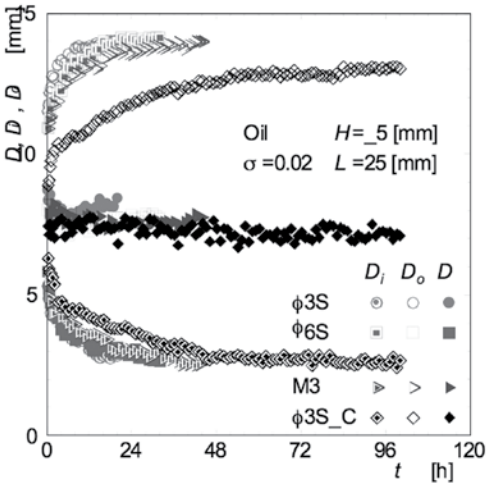

Figure 7. Erosion-ring diameters D, D_i, and D_o versus exposure time t for different nozzle outlets (H = –5 mm, L = 25 mm, σ = 0.02).

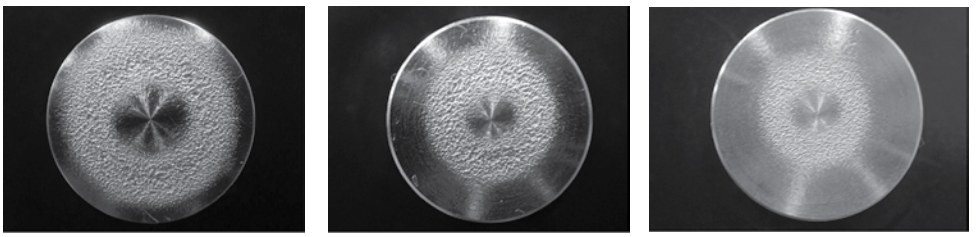

(a) σ = 0.02 (L = 25 mm) (b) σ = 0.03 (L = 22.5 mm) (c) σ = 0.04 (L = 20 mm)

Figure 8. Eroded surfaces of specimens for different nozzle outlets (ϕ3S, H = –10 mm, t = 8 h).

CONCLUSIONS

Experiments investigating cavitation erosion caused by impingement of oil jets were performed for different nozzle outlet geometries and impinged surface geometries. The effects of the geometries and cavitation number on the mass loss, erosion rate, surface damage, and erosion ring diameters of the specimens were examined. The results indicated that concave surfaces considerably reduced erosion. In this experiment, highering the cavitation number also produced a

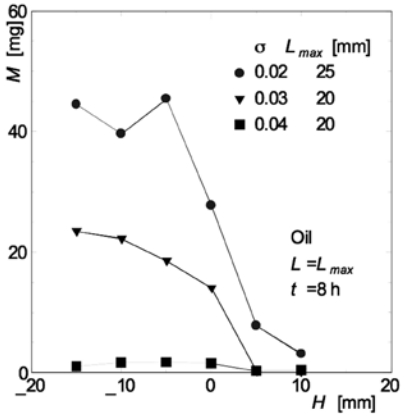

Figure 9. Effect of wall height H on mass loss M ($L = L_{max}$, t = 8 h).

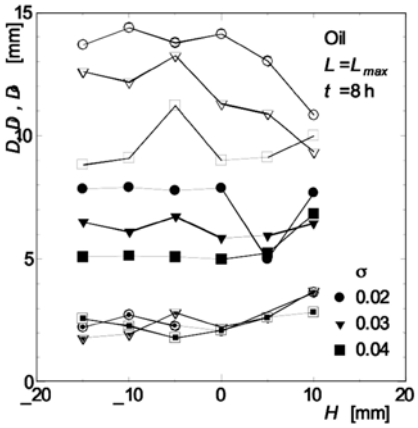

Figure 10. Effect of wall height H on erosion ring diameters D, D_i, and D_o ($L = L_{max}$, t = 8 h).

significant effect of reduction. In contrast, convex surfaces showed more erosion damage, but the mass loss and the characteristics of the eroded surfaces did not depend strongly on the amount of convexity. The results also indicate that mass loss was strongly influenced by the nozzle outlet geometry. In this experiment, the mass loss was reduced by elongating the flow path and by forming a small chamber at the nozzle outlet. Finally, the size of the ring-like eroded region was the smallest for concave specimen shapes and/or large cavitation numbers.

APPENDIX: NOMENCLATURE

D : Erosion ring diameter [mm]
ER : Mass loss rate [mg/h]
H : Height of cylindrical wall [mm]
L : Standoff distance [mm]

p_d : Downstream absolute pressure [MPa]
p_u : Upstream absolute pressure [MPa]
t : Exposure time [h]
σ : *Cavitation number* = p_d/p_u

ACKNOWLEDGMENT

The authors thank Messrs. Y. Miura, S. Isshiki, and R. Takahashi, among other former students of the Muroran Institute of Technology, for their cooperation in performing the experiments.

This paper was first presented in Proceedings of Thailand-Japan International Symposium in Industrial Engineering, Mechanical Engineering and Robotics 2010 (TJIEME-CMU-MuroranIT-2010).

REFERENCES

ASTM. 1995. Standard test method for erosion of solid materials by a cavitating liquid jet. Annual Book of ASTM Standards, G134.95: 529-540.

Kazama, T., K. Kumagai, Y. Miura, and Y. Narita. 2009. Reduction and enlargement of erosion by a submerged cavitating jet with geometric control. Proceedings of 9th Pacific Rim International Conference on Water Jetting Technology. pp.123-131, Sendai, Japan.

Kazama, T. and Y. Miura. 2007. Reduction in submerged jet cavitation erosion (Flow control by geometry close to nozzle outlets and impinged surfaces (in Japanese). Transactions of Japan Fluid Power System Society. 38, 6: 77-82.

Kazama, T. and K. Shimizu. 2007. Erosion due to impingement of submerged cavitating jets in tap water, biodegradable and mineral oils. Proceedings of 10th Scandinavian International Conference on Fluid Power, SICFP'07, pp. 91-105. Tampere, Finland.

Kazama, T. and A. Yamaguchi. 2000. Effects of configuration of nozzles, outlets of nozzles and specimens on erosion due to impingement of cavitating jet. Proceedings of 48th National Conference on Fluid Power, pp. 263-272, Las Vegas, USA.

Kleinbreuer, W. 1977. Kavitationserosion in hydraulischen systemen. Industrie-Anzeiger, 99, 34: 609-613.

Knapp, R.T., J.W. Daily, and F.G. Hammitt. 1970. Cavitation. McGraw-Hill.

Lichtarowicz, A. 1972. Use of a simple cavitating nozzle for cavitation erosion testing and cutting. Nature, Physical Science. 239, 91: 63-64.

Plesset, M.S. and R.E. Devine. 1966. Effect of exposure time on cavitation damage. Journal of Basic Engineering, Transactions of ASME, 88: 691-705.

Yamaguchi, A. and S. Shimizu. 1987. Erosion due to impingement of cavitating jet. Journal of Fluids Engineering, Transactions of ASME. 109, 4: 442-447.

Yamaguchi, A., T. Kazama, K. Inoue, and J. Onoue. 2001. Comparison of cavitation erosion test results between vibratory and cavitating jet methods. International Journal of Fluid Power. 2, 1: 25-30.

none